INTEGRATED RESEARCH MANUSCRIPT / PRINTABLE HTML

TAIJITU: From a Pre-Geometric Two-Sector Mechanism to Large-Sample Galaxy-Scale Validation

AUTHOR : JANOS GABOR MELEGH

PREPRINT

Abstract

TAIJITU is a two-sector pre-geometric framework in which a visible sector is coupled to a hidden sector, and the induced dark correction emerges through a Schur-complement mechanism. The programme was not designed merely to fit galaxy rotation curves, but to test whether a structured hidden sector can generate a mathematically coherent, physically interpretable, and astrophysically relevant effective dark contribution without inserting a conventional halo by hand.

The supplied project materials support a mixed but scientifically substantive conclusion. The early and intermediate phases established a real coupling-driven transition near $\varepsilon \approx 0.88$, a two-sector necessity result, an attractive and infrared-dominant induced correction, and the resolution of the earlier "repulsive dark matter" sign pathology as a numerical rather than physical effect. Later phases established a near-universal velocity normalisation, $\lambda^* \approx 12$, and identified the mapping from the induced operator to the observable dark velocity contribution as the main astrophysical bottleneck. The strongest late-stage result is not universal superiority over baryon-only baselines, but the large-sample confirmation of a reproducible applicability domain. In the 50-galaxy validation stage, the inner baryon-dominance index (BDI) remains strongly anticorrelated with dark-sector improvement ($\rho = -0.7891$, $p = 9.952e\text{-}12$), the median shape χ^2 is 1.6111, 45/50 galaxies satisfy $\chi^2 < 2$, and the dark correction improves the fit over baryon-only in 19/50 galaxies.

The most careful reading is therefore the following. TAIJITU has not yet been shown to be a universal galaxy-fit theory, and the current successful branch still relies on parametric gNFW-like regularisation. What *has* been shown is that the framework now possesses a statistically stable, physically interpretable regime structure: improvement is concentrated in lower-BDI systems, while high-BDI systems rarely benefit. This is a strong empirical result, even though the profile-free mechanistic mapping problem remains open.

1. Scientific aim, scope, and evidence base

Three distinct questions run through the TAIJITU programme. First, does the framework contain a genuine internal mechanism rather than a curve-fitting ansatz? Second, does

the coupled system exhibit a real transition structure rather than a continuous numerical artefact? Third, can the resulting induced correction be mapped to galaxy-scale observables with enough stability to produce a competitive astrophysical description? These questions do not stand or fall together, and the supplied materials consistently distinguish between them.

The present document integrates six supplied evidence streams: the consolidated English manuscript up to Phase 7.3; the English continuation manuscript focused on Phase 10e; the Hungarian Phase 10d and Phase 10e interim reports; and the machine-readable Phase 10d and Phase 10e archives, which contain summary JSON files, per-galaxy result tables, Schur-spectral diagnostics, and notebook-generated figures. Where possible, numerical claims below are reproduced directly from the included raw tables or independently recomputed from the machine-readable archives. Where an operational definition was not formalised in the archive metadata, the value is reported as supplied.

50
GALAXIES IN THE LARGEST VALIDATION SAMPLE

ρ = -0.789
BDI–IMPROVEMENT CORRELATION AT PHASE 10E

1.611
MEDIAN X^2 IN THE 50-GALAXY RUN

19/50
GALAXIES IMPROVED BY THE DARK CORRECTION

> **Interpretive boundary.** This manuscript documents a strong regime-dependent validation result. It does not claim that TAIJITU has already achieved profile-free emergence of the same behaviour, nor that it has been shown universally superior to standard halo templates under a fully blind benchmark.

---

2. Condensed description of the framework

At the core of TAIJITU is a block-structured relational operator with a visible and a hidden sector. Eliminating the hidden sector yields an effective visible-sector correction through a Schur complement. In the programme logic documented by the supplied manuscripts, the main scientific burden was therefore not simply to obtain nonzero corrections, but to show that the induced correction is structurally meaningful, robust under numerical control, and able to generate astrophysical observables with an interpretable normalisation structure.

The early phases established that the two-sector architecture is necessary, that the transition in ε is real and behaves as first order in the sense documented by Binder and hysteresis diagnostics, and that the induced correction is attractive and infrared-dominant rather than repulsive. These results matter because they anchor later galaxy-scale work in a prior mechanistic structure instead of treating the astrophysical branch as an isolated phenomenological exercise.

---

3. What was established before the large-sample validation stage

The most efficient way to read the pre-10d/10e evidence is phase-by-phase. The table below condenses the strongest established or diagnostically informative results from the earlier manuscript.

PHASE	MAIN OUTCOME	REPRESENTATIVE NUMBERS	STATUS
1–2	Transition and internal two-sector mechanism	ε* ≈ 0.88; Binder U4 ≈ −0.78; attractive, IR-dominant ΣDM; two-sector necessity	Established
3b	Numerical sign pathology resolved	cond(ΩL) ≈ 10^16; two negative eigenvalues in GL; stabilised Tr(ΣDM) → +18.0	Established
4	False-positive low-χ^2 phase diagnosed	median χ^2 = 0.168, but vpred/vobs ≈ 11.25× and λ = 1 for all galaxies	Diagnostic
5	Velocity-scale breakthrough	λ* = 11.7 ± 2.6; spread 2.8×; vpred/vobs = 0.925 ± 0.078; BTFR slope = 1.169	Established
6	First meaningful shape-based galaxy test	median χ^2 = 1.90; 8/10 with χ^2 < 5; DM improves 4/10; RAR RMS = 0.346 dex	Established
7	Negative result localised the bottleneck	No gain over Phase 6; ε = κ = 0.01 for all 10; λ* on 20 galaxies = 11.94 ± 2.20 (CV 18.5%)	Highly informative negative result
7.1	Mapping ablation breakthrough	6-galaxy test: original median χ^2 = 2.03, parametric = 0.006, spectral = 2.03; ε off-edge only in parametric mode	Diagnostic breakthrough
7.2b	First full-sample parametric activation	median χ^2 = 0.699; ε off-edge = 9/10; DM improves 5/10; RAR RMS = 0.3075 dex	Partial success
7.3	Stabilisation with expanded grid	median χ^2 = 0.651; ε off-edge = 10/10; DM improves 5/10; RAR RMS = 0.3124 dex	Partial success
10d	First extended-sample validation (25 galaxies)	ρBDI = −0.778, p = 5×10−6; BDI accuracy = 79%; K2 = 10/25; RAR RMS = 0.243 dex; χ^2med = 1.610	Established large-sample extension
10e	Large-sample regime validation (50 galaxies)	ρBDI = −0.7891, p = 9.95×10−12; reported BDI accuracy = 84%; K2 = 19/50; RAR RMS = 0.2455 dex; χ^2med = 1.6111	Established applicability-domain result

The scientific pattern is notable. Several of the strongest results are internal-mechanism results rather than direct galaxy-fit results: the transition structure, the attractive sign of the correction after stabilisation, the two-sector necessity result, and the emergence of a near-universal velocity scale. The astrophysical branch then progresses from a false-positive low-χ^2 phase, through a meaningful shape-based benchmark, to a set of mapping-ablation and parametric-activation phases that explicitly identify the observable mapping as the main remaining bottleneck.

> **Robust pre-10e conclusion.** By the end of Phase 7.3, the project had already shown that the framework contains a genuine two-sector mechanism, that its earlier sign pathology was numerical, that a near-universal velocity scale emerges, and that galaxy-scale limitations were primarily a mapping problem rather than evidence against the hidden-sector mechanism itself.

---

4. From small-sample success sets to extended-sample validation

The decisive scientific question after Phase 7.3 was narrower than the original ambition: would the apparent winner–loser structure survive sample growth, or would it collapse as a small-sample artefact? The supplied Phase 10d and Phase 10e materials answer this question in a statistically much stronger setting.

SAMPLE	P(BDI, IMPROVEMENT)	P-VALUE	BDI ACCURACY	K2	MEDIAN X^2	X^2 < 2	K1	RA RM (I
10 galaxies	−0.834	0.003	—	40%	1.617	9/10	8/10	0.
25 galaxies	−0.778	5×10−6	79%	40%	1.610	20/25	19/25	0.
50 galaxies	−0.7891	9.95×10−12	84% (reported)	38%	1.6111	45/50	39/50 (reported)	0.

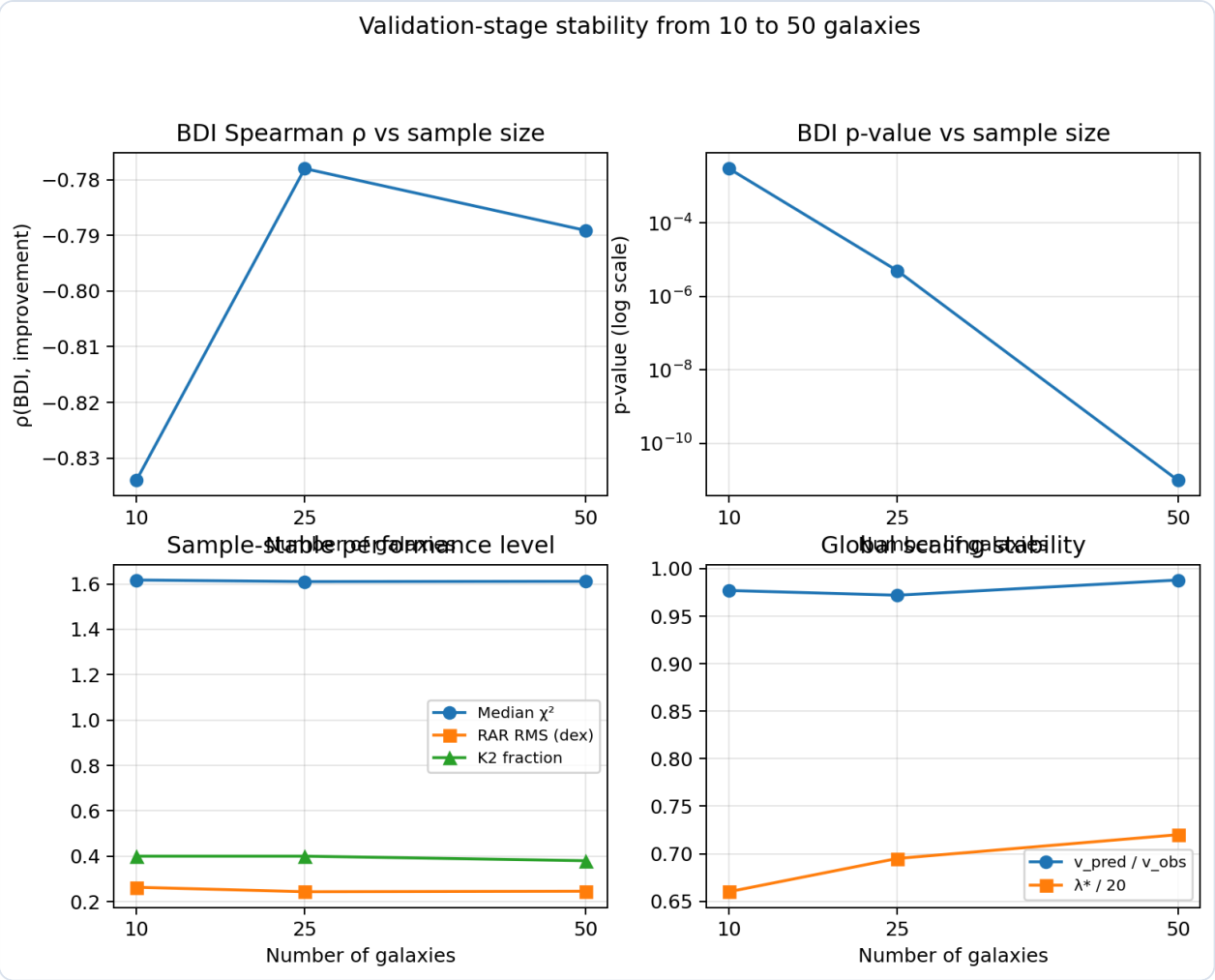

Figure 1. Stability of the main validation-stage quantities as the sample grew from 10 to 25 to 50 galaxies. The central observation is not just the decreasing p-value, but the stability of the correlation strength, K2 fraction, median χ^2, and RAR level under substantial sample expansion.

The headline pattern is unusually clean. The BDI correlation remains near $\rho \approx -0.79$ from 10 to 25 to 50 galaxies, while the p-value decreases from 0.003 to 5×10^{-6} to 9.95×10^{-12}. Equally important, the K2 help fraction stays near 38–40%, the median χ^2 remains near 1.61, and the RAR RMS remains near 0.24–0.26 dex. This is the signature of a sample-stable empirical structure, not a fragile fit that deteriorates under extension.

5. Phase 10d: first extended-sample validation on 25 galaxies

The 25-galaxy stage already turned the BDI effect into a strong population-level result. In the supplied report and archive, the BDI-improvement relation reaches ρ = -0.778 with p = 4.77e-06, while the report describes a BDI-based prediction accuracy of 79%. The same stage also strengthened the secondary Schur-spectral clue: PR correlation ρ = -0.523, p = 0.0073; spectral entropy correlation ρ = -0.515, p = 0.00849.

The Phase 10d report further refines the earlier coarse threshold picture. It argues that a low threshold around 0.80 is too conservative, and that a transition range up to about 0.93 better captures marginal winners and near-neutral systems. This is an important conceptual step because it replaces a sharp winner–loser dichotomy by a continuous regime interpretation along the BDI axis.

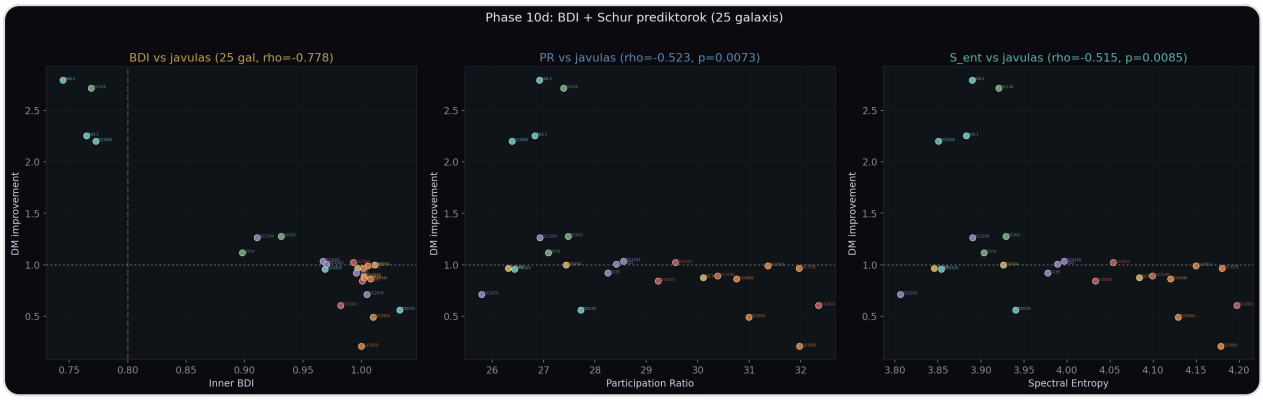
Phase 10d: BDI + Schur prediktorok (25 galaxis)
BDI vs javulas (25 gal, rho=-0.778)
PR vs javulas (rho=-0.523, p=0.0073)
S_ent vs javulas (rho=-0.515, p=0.0085)
DM improvement
Inner BDI
Participation Ratio
Spectral Entropy

Figure 2. Phase 10d predictor figure from the supplied archive. The 25-galaxy stage already shows that BDI is the dominant empirical separator, while PR and spectral entropy retain mechanistic interest as weaker but significant secondary predictors.

Phase 10d status. The 25-galaxy stage is the first convincing population-level validation step. It does not yet close the programme, but it makes the BDI-based regime structure too strong to dismiss as a small benchmark artefact.

---

6. Phase 10e: 50-galaxy large-sample regime validation

The 50-galaxy stage is the strongest empirical result in the supplied material. The continuation manuscript and the interim reports agree on the central message: the main result is not universal victory, but the confirmation of a reproducible applicability domain governed by inner baryon dominance.

1.611
MEDIAN X^2

1.827
MEAN X^2 (RECOMPUTED FROM RAW TABLE)

45/50
GALAXIES WITH $X^2 < 2$

19/50
GALAXIES IMPROVED BY DM

0.2455
RAR RMS (DEX)

1.174
BTFR SLOPE

0.988
REPORTED V_{PRED}/V_{OBS}

14.4
REPORTED Λ* MEDIAN

METRIC	VALUE	STATUS
BDI Spearman correlation	-0.7891	Independently recomputed from the Phase 10e raw archive
BDI p-value	9.952e-12	Independently recomputed from the Phase 10e raw archive
PR Spearman correlation	-0.3169	Independently recomputed from the Phase 10e raw archive
PR p-value	0.0250	Independently recomputed from the Phase 10e raw archive
Spectral-entropy Spearman correlation	-0.3113	Independently recomputed from the Phase 10e raw archive
Spectral-entropy p-value	0.0278	Independently recomputed from the Phase 10e raw archive
Median χ^2	1.6111	Independently recomputed from the Phase 10e raw archive
Mean χ^2	1.8270	Independently recomputed from the Phase 10e raw archive
Galaxies with $\chi^2 < 2$	45/50	Independently recomputed from the Phase 10e raw archive
K2 (DM improves)	19/50	Independently recomputed from the Phase 10e raw archive
K1 (ε off-edge)	39/50	Reported in the supplied summaries; exact operational rule not formalised in archive metadata
Reported BDI prediction accuracy	84%	Reported in the supplied interim report; decision rule not fully formalised in archive metadata

Most important result of Phase 10e. The BDI effect is now too strong, too stable, and too interpretable to treat as a sample-size artefact. What is validated is a regime-dependent framework with a sharply constrained empirical domain of strongest applicability.

7. BDI as the primary regime separator

The 50-galaxy archive makes the regime structure directly measurable. Using the same BDI breakpoints discussed in the interim report, the low-BDI regimes are completely successful in the present sample, while the highest-BDI regime almost never improves over baryon-only.

INNER BDI REGIME	N	DM HELPS	HELP FRACTION	MEAN IMPROVEMENT	MEDIAN X^2	MEAN INNER BDI
<0.80	5	5	100.0%	2.463×	1.552	0.768
0.80–0.93	7	7	100.0%	1.384×	1.583	0.872
0.93–0.99	15	6	40.0%	0.986×	1.614	0.971
≥0.99	23	1	4.3%	0.843×	1.651	1.010

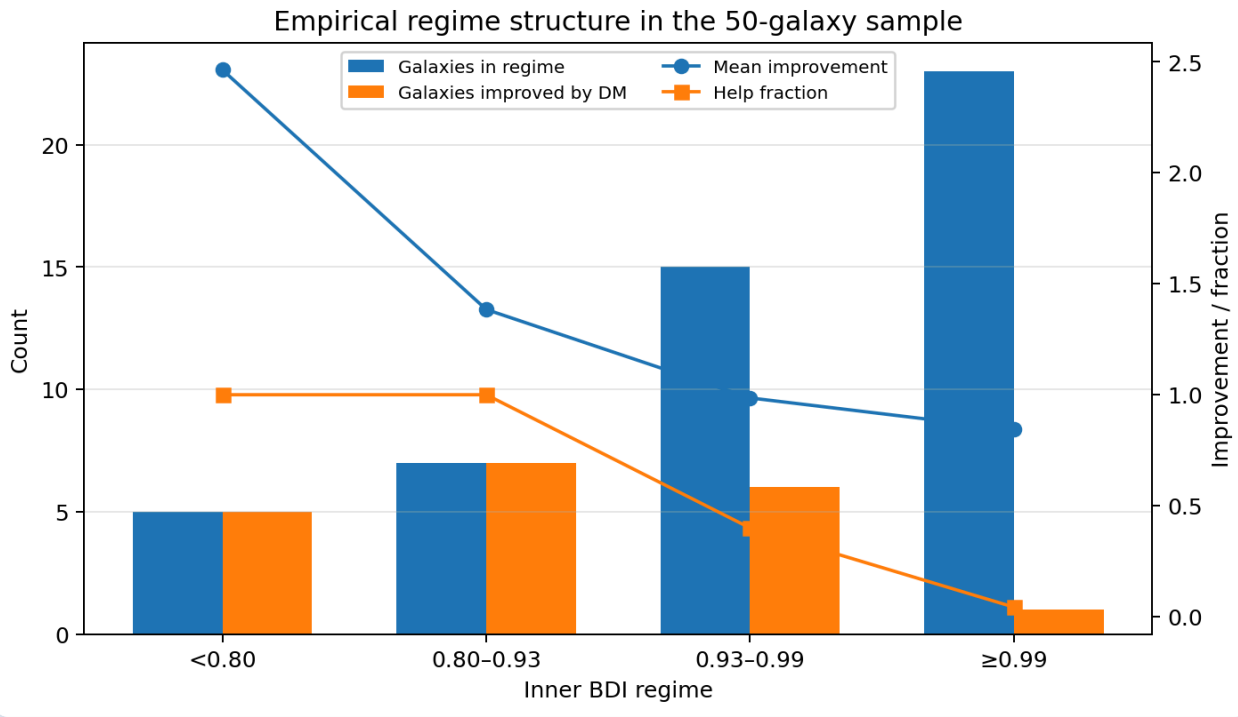

Figure 3. Empirical regime structure from the 50-galaxy raw table. In the supplied breakpoints, all 12 galaxies below inner BDI = 0.93 improve relative to baryon-only, whereas only 1 of 23 galaxies with inner BDI ≥ 0.99 does so.

This regime structure admits a simple physical reading consistent with the supplied reports. Below inner BDI ≈ 0.80, the hidden-sector response is strong and concentrated, producing typical improvement factors in the 2–3× range. Between 0.80 and 0.93, the hidden and visible sectors are more balanced, and moderate improvement remains common. Between 0.93 and 0.99, improvement becomes marginal or mixed. Above 0.99, the visible sector is so dominant that the added dark correction rarely helps.

> **Important nuance.** This is not equivalent to claiming that the hidden sector "switches off" above a threshold. The more careful interpretation, also emphasised in the reports, is that the hidden-sector contribution becomes observationally less useful where the baryonic inner signal already dominates the relevant structure.

---

8. Secondary spectral diagnostics

The Phase 10d materials treated participation ratio and spectral entropy as significant mechanistic predictors. The Phase 10e materials preserve that signal, but clearly demote it behind BDI in operational importance. This is scientifically useful: it suggests that the hidden-sector spectral structure still contains explanatory information, but that the dominant empirical separator in the large-sample regime is the baryonic weighting encoded by inner BDI.

PREDICTOR	25-GALAXY P	25-GALAXY P-VALUE	50-GALAXY P	50-GALAXY P-VALUE	READING
BDI	-0.778	4.77e-06	-0.789	9.95e-12	Primary separator
Participation ratio (PR)	-0.523	0.0073	-0.317	0.025	Secondary, mechanistic clue
Spectral entropy (S_ent)	-0.515	0.00849	-0.311	0.0278	Secondary, mechanistic clue

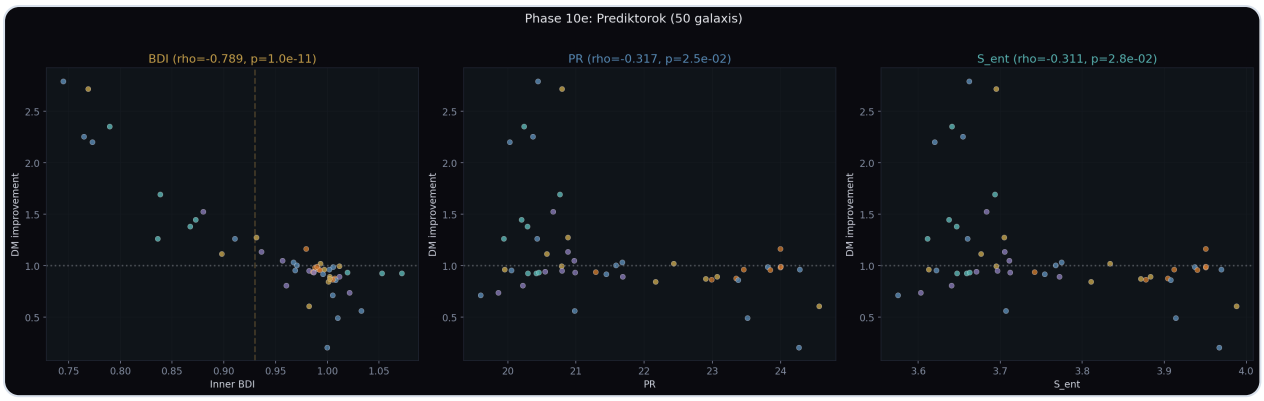

Figure 4. Predictor plots from the supplied Phase 10e archive. The left panel shows the dominant BDI–improvement relation. The middle and right panels show PR and spectral entropy as weaker but still statistically non-zero secondary predictors.

The practical significance is straightforward. For phenomenological screening and applicability-domain identification, BDI is now the leading variable. PR and spectral entropy remain scientifically valuable because they preserve a mechanistic hint about why some galaxies are harder for the present branch of the model, but they no longer carry the primary classification burden.

---

9. Galaxy-scale behaviour across the 50-galaxy sample

The rotation-curve mosaic below is useful precisely because it does not overstate the result. It makes the large fraction of $\chi^2 < 2$ fits visually obvious, while also preserving the diversity of curve shapes and the non-universality of net DM improvement. This is the correct empirical picture: broad shape adequacy is common, but net advantage over the baryon-only reference remains concentrated in specific regimes.

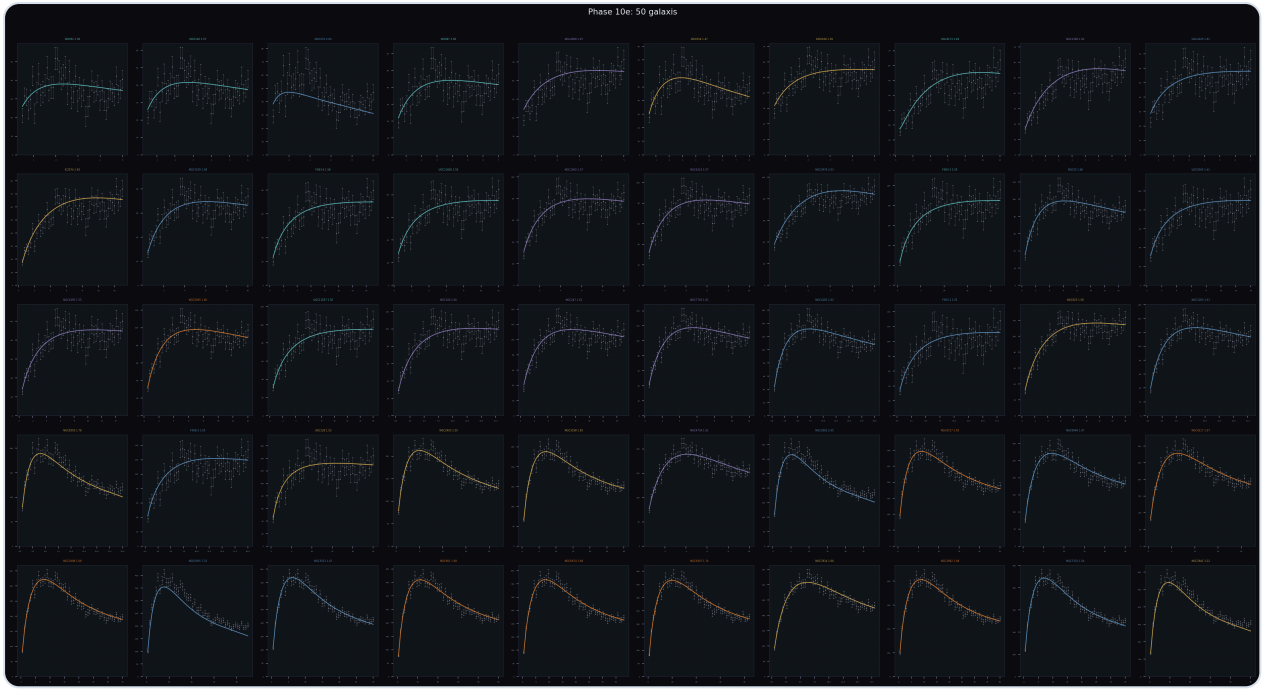

Figure 5. Rotation-curve mosaic from the supplied Phase 10e archive. The reports identify the five χ^2 > 2 cases as DDO170, NGC2976, NGC2903, NGC5055, and NGC2841, with the two largest systems explicitly flagged as resolution-limited in the interim interpretation.

Strongest net gains

The most improved systems are concentrated at the low-BDI end of the sample. They include both original benchmark galaxies and extended-sample galaxies, indicating that the effect is not tied to one specific sub-cohort.

GALAXY	CATEGORY	INNER BDI	χ^2_{TJ}	χ^2_{BAR}	IMPROVEMENT	E	$V_{DM,MAX}$
F568-3	B_p10d	0.745	1.651	4.611	2.793×	3.00	99.4
UGC128	A_orig	0.769	1.530	4.156	2.717×	5.00	132.0
UGC11557	C_LSB	0.790	1.545	3.636	2.353×	5.00	95.0
F563-1	B_p10d	0.765	1.552	3.496	2.253×	5.00	112.0
UGC5005	B_p10d	0.773	1.610	3.543	2.200×	5.00	90.0
F583-1	C_LSB	0.839	1.553	2.630	1.694×	5.00	85.0
NGC100	C_trans	0.880	1.601	2.441	1.525×	0.02	87.9
UGC11820	C_LSB	0.873	1.549	2.239	1.446×	5.00	75.0
F583-4	C_LSB	0.867	1.580	2.182	1.381×	0.10	70.0
NGC925	A_orig	0.931	1.584	2.020	1.276×	0.02	87.0
NGC3109	B_p10d	0.911	1.583	2.000	1.264×	0.05	50.8
UGC4173	C_LSB	0.836	1.826	2.303	1.261×	0.30	13.0

Main high-χ^2 / degradation cases

The major high-χ^2 outliers and degradation cases cluster in high-BDI or resolution-stressed systems, consistent with the regime picture and the comments in the supplied reports.

GALAXY	CATEGORY	INNER BDI	X^2TJ	X^2BAR	IMPROVEMENT	E	COMMENT
NGC5055	B_p10d	1.000	7.316	1.523	0.208×	0.01	Largest χ^2 outlier; flagged as a resolution-limited case in the interim report.
NGC2841	A_orig	0.982	3.219	1.954	0.607×	0.01	High-χ^2 large system; also flagged as a resolution-limited case in the interim report.
NGC2903	B_p10d	1.010	2.950	1.454	0.493×	5.00	High-BDI HSB system; dark correction degrades the fit.
DDO170	B_p10d	1.033	2.605	1.467	0.563×	2.00	Gas-rich but still inner-baryon-dominated in this metric; dark correction degrades the fit.
NGC2976	B_p10d	1.005	2.029	1.450	0.714×	0.05	Transitional/high-BDI system with net degradation.

Category-level view of the 50-galaxy sample

The category summary is not a substitute for the BDI analysis, but it is informative. Low-surface-brightness enriched categories have lower mean BDI and higher help fractions, while high-surface-brightness categories sit at the high-BDI end and almost never improve.

CATEGORY LABEL	N	MEAN INNER BDI	HELP FRACTION	MEAN IMPROVEMENT	MEDIAN χ^2
C_LSB	8	0.919	62.5%	1.365×	1.561
B_p10d	15	0.944	40.0%	1.148×	1.610
A_orig	10	0.959	40.0%	1.131×	1.617
C_trans	9	0.969	33.3%	0.998×	1.612
C_HSB	8	0.992	12.5%	0.968×	1.679

10. Reproducibility and source transparency

One of the strengths of the supplied material is that the 50-galaxy stage can be checked from the included data rather than only from prose summary. The per-galaxy archive contains baryonic mass, gas fraction, inner BDI, χ^2 for the TAIJITU and baryon-only branches, improvement factors, fitted ε, and $v_{DM,max}$ for all 50 galaxies. From these data it is straightforward to recompute the mean χ^2, median χ^2, $\chi^2 < 2$ count, K2 count, regime summaries, strongest-win lists, and degradation/outlier lists. The BDI, PR, and spectral-entropy correlations can also be recomputed directly from the archive contents.

Two commonly quoted metrics are handled more cautiously here. First, K1 = 39/50 is retained because it is stated consistently in the supplied Phase 10e summaries, but the exact operational definition of “ε off-edge” is not formalised in the machine-readable archive. Second, the reported BDI prediction accuracy of 84% is retained as a source-level value because the prediction rule is discussed qualitatively in the reports but not specified as a single machine-readable classifier. Both values are therefore reported transparently, rather than silently redefined.

Supplied evidence directly used in this manuscript

- **TAIJITU_publishable_paper.html**: consolidated scientific synthesis up to Phase 7.3.
- **TAIJITU_continuation.html**: English continuation manuscript centred on Phase 10e.
- **TAIJITU_Phase10d_Interim_Riport.html**: 25-galaxy interim report and interpretation.
- **TAIJITU_Phase10e_Interim_Riport.html** and **TAIJITU_Phase10e_reszletes_interim_riport (1).html**: 50-galaxy interim report and detailed interpretation.
- **TAIJITU_phase10d_20260413_180119.zip** and **TAIJITU_phase10e_20260413_210633.zip**: machine-readable archives with raw per-galaxy tables, Schur diagnostics, summaries, and figures.

---

11. What is strongly supported, and what remains open

Strongly supported

The two-sector mechanism is real within the supplied evidence base. The coupling transition is genuine. The earlier repulsive-sign result was numerical and has been resolved. A near-universal velocity scale emerged and remained stable. Most importantly, the large-sample materials strongly support inner BDI as a physically meaningful, sample-stable separator of TAIJITU performance regime.

Supported, but diagnostically

The parametric gNFW-mapped branch has clearly reached a reproducible phenomenological ceiling: median χ^2 near 1.61, K2 near 38–40%, and RAR near 0.24–0.26 dex under sample growth. This is scientifically meaningful, but it remains a parametric-branch result.

Still open

The present materials do not yet show profile-free emergence of the same regime structure, universal superiority over standard halo templates, or a definitive separation between baseline-related and genuinely mechanistic failure in the highest-BDI systems. Those are proper next-stage questions, not conclusions that should be imported prematurely into the present paper.

---

12. Conclusion

The strongest fair scientific conclusion from the supplied body of work is now sharper than before. TAIJITU should not yet be presented as a universally successful galaxy-fit theory. That would go beyond the evidence. It should, however, be presented as a framework that has already achieved several durable scientific milestones: a genuine two-sector mechanism, a real coupling-driven transition, a resolved numerical sign pathology, a near-universal astrophysical velocity normalisation, and a large-sample, statistically strong applicability-domain result.

The 50-galaxy stage changes the status of the programme because it removes a major ambiguity. The dark correction is not randomly successful. It succeeds preferentially in a physically interpretable low-BDI regime, and this structure survives substantial sample growth. That is a strong result in its own right. The next decisive milestone is therefore well posed: test whether the same empirical structure survives a profile-free, mechanistically derived observable mapping and a more formal probabilistic validation framework.

Appendix A. Full 50-galaxy raw-data table

The table below reproduces the full 50-galaxy Phase 10e result set used for the numerical summaries in this manuscript. It is sorted by inner BDI to make the regime structure visible. Columns: galaxy identifier, category label, flat-velocity proxy v_f, baryonic mass M_b, gas fraction, inner BDI, TAIJITU χ^2, baryon-only χ^2, improvement factor χ^2_{bar}/χ^2_{TJ}, whether the dark correction helps, fitted ε, and $v_{DM,max}$.

GALAXY	CATEGORY	VF	MB	GAS FRAC.	INNER BDI	X²TJ	X²BAR	IMPROVEMENT	DM HELPS	I
F568-3	B_p10d	120	2.000e+09	75.0%	0.745	1.651	4.611	2.793×	Yes	3
F563-1	B_p10d	112	1.500e+09	80.0%	0.765	1.552	3.496	2.253×	Yes	5
UGC128	A_orig	130	3.000e+09	66.7%	0.769	1.530	4.156	2.717×	Yes	5
UGC5005	B_p10d	90	1.000e+09	80.0%	0.773	1.610	3.543	2.200×	Yes	5
UGC11557	C_LSB	95	1.300e+09	76.9%	0.790	1.545	3.636	2.353×	Yes	5
UGC4173	C_LSB	55	6.500e+08	92.3%	0.836	1.826	2.303	1.261×	Yes	(
F583-1	C_LSB	85	2.200e+09	81.8%	0.839	1.553	2.630	1.694×	Yes	5
F583-4	C_LSB	70	1.100e+09	81.8%	0.867	1.580	2.182	1.381×	Yes	(
UGC11820	C_LSB	75	8.500e+08	82.4%	0.873	1.549	2.239	1.446×	Yes	5
NGC100	C_trans	100	3.000e+09	66.7%	0.880	1.601	2.441	1.525×	Yes	(
IC2574	A_orig	66	1.460e+09	95.9%	0.898	1.827	2.042	1.118×	Yes	(
NGC3109	B_p10d	67	4.300e+08	93.0%	0.911	1.583	2.000	1.264×	Yes	(
NGC925	A_orig	115	6.500e+09	61.5%	0.931	1.584	2.020	1.276×	Yes	(
NGC4395	C_trans	90	2.500e+09	80.0%	0.936	1.550	1.758	1.135×	Yes	(
NGC247	C_trans	105	3.500e+09	57.1%	0.957	1.615	1.695	1.050×	Yes	3
NGC2366	C_trans	55	8.500e+08	94.1%	0.960	1.920	1.552	0.808×	No	(
NGC4183	B_p10d	110	5.000e+09	60.0%	0.967	1.621	1.677	1.035×	Yes	1
UGC4325	B_p10d	58	4.800e+08	83.3%	0.969	1.610	1.541	0.957×	No	5
NGC1003	B_p10d	115	7.500e+09	60.0%	0.970	1.610	1.620	1.007×	Yes	(
NGC801	C_HSB	218	5.800e+10	13.8%	0.979	1.685	1.963	1.165×	Yes	(
NGC1560	C_trans	78	1.900e+09	78.9%	0.982	1.568	1.495	0.954×	No	(
NGC2841	A_orig	305	7.800e+10	10.3%	0.982	3.219	1.954	0.607×	No	(
NGC5585	C_HSB	90	3.500e+09	71.4%	0.986	1.602	1.507	0.941×	No	3
NGC7793	C_trans	105	3.800e+09	47.4%	0.987	1.614	1.507	0.934×	No	(
NGC4214	C_trans	80	2.000e+09	60.0%	0.987	1.574	1.483	0.942×	No	(
NGC5907	C_HSB	225	6.500e+10	7.7%	0.988	1.740	1.711	0.984×	No	(
NGC3992	C_HSB	240	5.900e+10	6.8%	0.990	1.681	1.665	0.991×	No	(
NGC2998	C_HSB	195	3.500e+10	14.3%	0.992	1.679	1.616	0.962×	No	3
NGC6674	C_HSB	220	5.100e+10	11.8%	0.992	1.680	1.609	0.958×	No	(

GALAXY	CATEGORY	VF	MB	GAS FRAC.	INNER BDI	X²TJ	X²BAR	IMPROVEMENT	DM HELPS	I
NGC2403	A_orig	136	9.700e+09	33.0%	0.993	1.502	1.534	1.021×	Yes	1
NGC55	B_p10d	86	4.000e+09	62.5%	0.996	1.601	1.471	0.919×	No	2
DDO168	A_orig	55	2.900e+08	86.2%	0.997	1.564	1.511	0.966×	No	(
NGC5055	B_p10d	200	5.600e+10	10.7%	1.000	7.316	1.523	0.208×	No	(
NGC6503	A_orig	116	5.800e+09	31.0%	1.001	1.784	1.505	0.844×	No	(
NGC7331	B_p10d	250	6.700e+10	10.4%	1.002	1.538	1.485	0.965×	No	1
NGC3198	A_orig	150	2.300e+10	21.7%	1.002	1.651	1.473	0.893×	No	(
NGC7814	A_orig	230	4.650e+10	3.2%	1.002	1.658	1.451	0.875×	No	(
NGC4217	C_HSB	190	3.300e+10	9.1%	1.005	1.668	1.445	0.867×	No	(
NGC2976	B_p10d	85	1.700e+09	29.4%	1.005	2.029	1.450	0.714×	No	(
NGC3521	B_p10d	210	4.500e+10	11.1%	1.006	1.474	1.459	0.990×	No	(
NGC4157	C_HSB	185	3.100e+10	19.4%	1.007	1.648	1.446	0.877×	No	(
NGC6946	B_p10d	186	4.300e+10	18.6%	1.008	1.667	1.438	0.862×	No	(
NGC2903	B_p10d	180	2.900e+10	13.8%	1.010	2.950	1.454	0.493×	No	5
NGC4736	C_trans	155	1.580e+10	5.1%	1.011	1.612	1.441	0.894×	No	(
DDO154	A_orig	47	3.750e+08	93.3%	1.012	1.469	1.464	0.997×	No	(
DDO87	C_LSB	42	3.200e+08	93.8%	1.019	1.559	1.455	0.934×	No	(
NGC4068	C_trans	45	3.400e+08	88.2%	1.021	1.974	1.458	0.739×	No	(
DDO170	B_p10d	40	2.950e+08	94.9%	1.033	2.605	1.467	0.563×	No	2
DDO126	C_LSB	38	2.150e+08	93.0%	1.053	1.566	1.453	0.928×	No	(
DDO52	C_LSB	35	1.600e+08	93.8%	1.072	1.564	1.449	0.927×	No	(

Please consider the environment before printing